

Synthesis, molecular docking and ADMET properties of ethyl 4-[3-(ethoxycarbonyl)-1-phenyl-1*H*-pyrazol-4-yl]-2-oxo/thioxo-1,2,3,4-tetrahydropyrimidine-5-carboxylates as potential antiparasitic agents

Yevhen Nefedov^a, Natalia Darmograi^b, Mykola Obushak^a and Vasyl Matychuk^{a*}

^aDepartment of Organic Chemistry, Ivan Franko National University of Lviv, Kyryla and Mefodiya St. 6, Lviv 79005, Ukraine

^bDepartment of Toxicological and Analytical Chemistry, Danylo Halytsky Lviv National Medical University, Pekarska St. 69, Lviv 79010, Ukraine

CHRONICLE

Article history:

Received March 22, 2025

Received in revised form

June 19, 2025

Accepted August 21, 2025

Available online

August 21, 2025

Keywords:

Biginelli Reaction

Pyrazole

Tetrahydropyrimidines

Molecular Docking

ADMET

DHFR

Leishmania

Trypanosoma Cruzi

ABSTRACT

The method for the synthesis of ethyl 4-[3-(ethoxycarbonyl)-1-phenyl-1*H*-pyrazol-4-yl]-2-oxo/thioxo-1,2,3,4-tetrahydropyrimidine-5-carboxylates was developed, and the bioactivity of the obtained compounds against infectious agents was predicted. Docking studies of the synthesised compounds were performed on pteridine reductase 1 (PTR1) of *Leishmania*, dihydrofolate reductase–thymidylate synthase of *Trypanosoma cruzi*, and human dihydrofolate reductase. The results demonstrated that the investigated compounds exhibit high affinity for these enzymes. Moderate selectivity relative to human DHFR was also observed. In addition, the predicted drug-likeness, ADME-Tox parameters, and toxicity profiles suggest the potential of the synthesised compounds for further pharmacological development.

© 2025 by the authors; licensee Growing Science, Canada.

1. Introduction

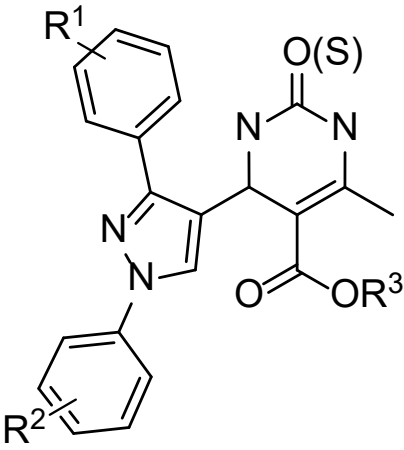
The Biginelli reaction is a classical multicomponent transformation employed in the synthesis of 3,4-dihydropyrimidin-2(1*H*)-ones. It is a straightforward one-pot condensation involving an aromatic aldehyde, urea or thiourea, and a β -ketoester in a single step. Notably, 3,4-dihydropyrimidin-2(1*H*)-ones serve as valuable scaffolds for the post-synthetic modification into diverse heterocyclic derivatives.¹⁻⁴

Multicomponent reactions offer several advantages, including the use of simple starting materials, operational simplicity, and access to structurally complex products, which explains the growing interest in such methodologies.⁵⁻⁸ In particular, these reactions have proven effective for the rapid synthesis of structurally diverse molecular libraries, which is of great relevance to medicinal chemistry and drug discovery.⁹ Substituted aromatic and heteroaromatic aldehydes, including pyrazole-4-carbaldehydes, have been extensively explored in this context, affording hybrid molecules bearing both dihydropyrimidinone and pyrazole moieties. These two frameworks are widely recognised as privileged scaffolds in drug design, and their combination is believed to enhance pharmacological properties through synergistic effects. In the present study, 1,3-diaryl-1*H*-pyrazole-4-carbaldehydes were employed in a modified Biginelli reaction to afford ethyl 6-methyl-2-oxo-4-(1*H*-pyrazol-4-yl)-1,2,3,4-tetrahydropyrimidine-5-carboxylate derivatives (**A**). The biological activities of the synthesised compounds have been evaluated (see **Table 1**).¹⁰⁻¹⁸

* Corresponding author

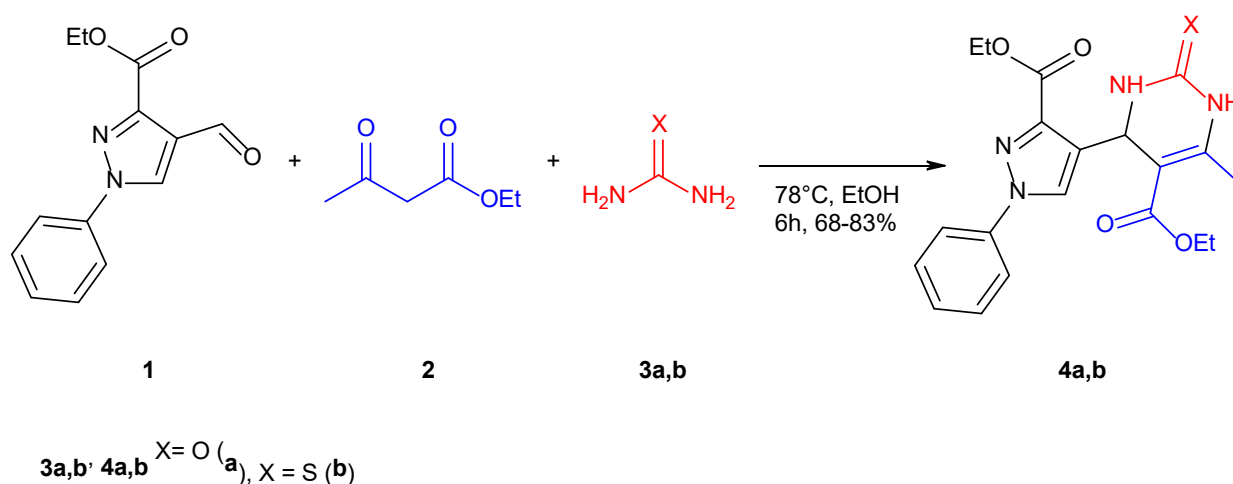
E-mail address v.matychuk@ukr.net (V. Matychuk)

Table 1. Bioactive Dihydropyrimidinone–Pyrazole Derivatives.

Compounds	Reported Biological Activity	Reference
 <p style="text-align: center;">A</p>	antiprolifative	10
	antimalarial	11
	antimicrobial	12, 13
	antioxidant	12
	antitubercular	14, 15
	anticancer	15
	antiinflammatory	16
	calcium channel blockers	17
	insecticidal	18
	anti-biofilm	13

2. Results and Discussion

The aim of this work is to synthesise novel Dihydropyrimidinone–Pyrazole Derivatives and to predict their biological activity, pharmacokinetic parameters, and toxicity. The target compounds were obtained via multicomponent reactions of ethyl 4-formyl-1-phenyl-1*H*-pyrazole-3-carboxylate **1**, ethyl acetoacetate **2**, and urea or thiourea **3a,b** in refluxing ethanol.



Scheme 1. Synthesis of compounds **4a,b**.

The structures of the obtained compounds were established by ¹H-NMR spectroscopy and elemental analysis (see Experimental section).

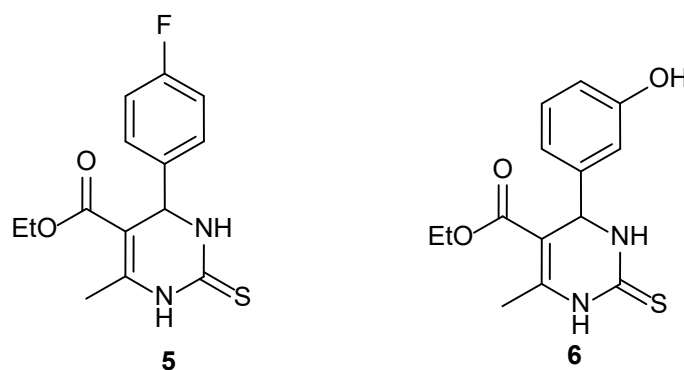


Fig. 1. Structures of 3,4-dihydropyrimidin-2(1*H*)-thiones – inhibitors of Dihydrofolate reductase.

Using an online predictive tool,¹⁹ the biological activity of compounds **4a** and **4b** was assessed with a focus on infectious agents. The analysis indicated a high probability of antiprotozoal activity, particularly against the pathogens responsible for Chagas disease (*Trypanosoma cruzi*) and species of the *Leishmania* genus. These diseases pose significant therapeutic challenges, especially in tropical and subtropical regions. Dihydrofolate reductase (DHFR) is a well-established target in their treatment, as it plays a crucial role in folate metabolism and, consequently, in cell proliferation. Notably, the effective DHFR-inhibitory activity of 3,4-dihydropyrimidin-2(1*H*)-thiones (see **Fig. 1**), including compounds **5** and **6** (Monastrol), has been previously reported.²⁰

One of the most important enzymes involved in the metabolism of the aforementioned pathogens is pteridine reductase 1 (PTR1) from *Leishmania* and dihydrofolate reductase–thymidylate synthase (DHFR-TS) from *Trypanosoma cruzi*. We determined the binding affinities and predicted the protein–ligand binding conformations within the active sites of LdPTR1 and TcDHFR-TS. Potential drug candidates capable of binding to and inhibiting these enzymes can be identified through molecular docking studies. The binding affinities of compounds **4a** and **4b** for these enzymes range from -7.1 to -8.5 kcal/mol, comparable to the known dihydrofolate reductase inhibitor methotrexate. The results are summarized in **Table 2**. Docking studies were also performed for the binding of compounds **4a** and **4b** to human DHFR, revealing binding affinities of -6.7 and -6.6 kcal/mol, respectively. Moderate selectivity of the synthesised compounds towards *Leishmania* PTR1 and *Trypanosoma cruzi* DHFR-TS was observed (see **Table 2**).

Table 2. Binding affinities of compounds **4a** and **4b** (kcal/mol).

Compound	LdPTR1	TcDHFR-TS	Human DHFR
4a	-7.1	-8.1	-6.7
4b	-8.5	-7.6	-6.6
Methotrexate	-8.5	-9.5	-9.0

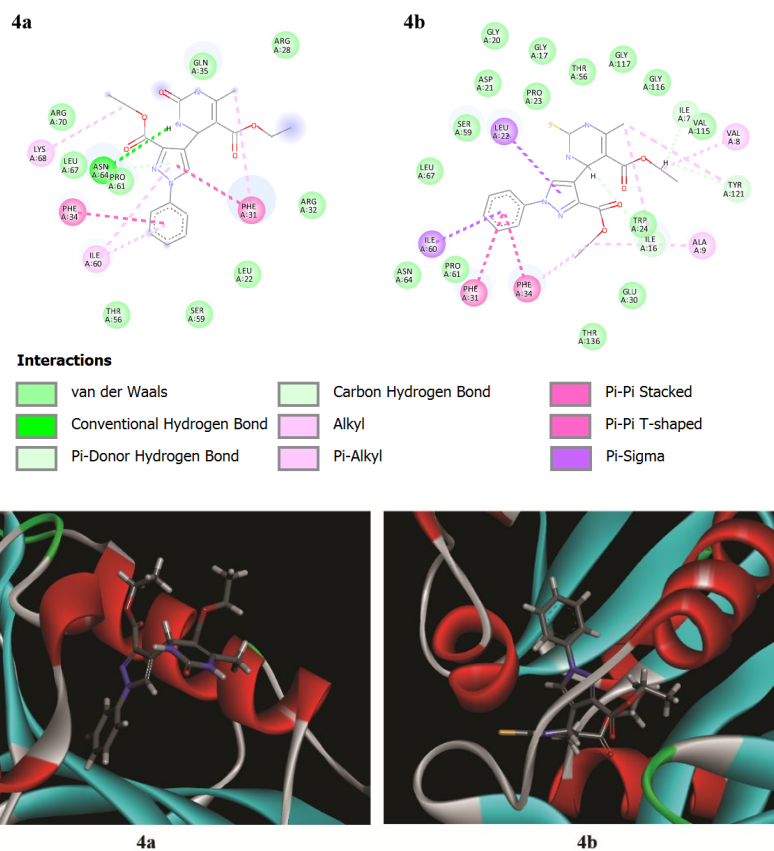
The binding of ligands **4a** and **4b** to the studied enzymes involves strong hydrogen bonds, as shown in **Table 3**. In the case of LdPTR1, π - π interactions involving the phenylalanine residue of the protein contribute significantly to the binding of the compounds within the active site. Compound **4b** is characterised by an interaction between the π -system of the imidazole ring of His A:38 and the p-orbital of the sulfur atom at the C-2 position of the 1,2,3,4-tetrahydropyrimidine ring.

Table 3. Protein-ligand interactions.

Compound	Hydrogen Bond	Interactions involved Pi systems	Hydrophobic interactions	Van der Waals interactions
LdPTR1 (PDBID: 2XOX), (Leishmaniasis)				
4a	Asn A:64 (Conventional) Asn A:64 (Pi-Donor)	Phe A:34 (Pi-Pi) Phe A:31 (Pi-Pi)	Lys A:68 Ile A:60 Phe A:31	Arg A:70 Leu A:67 Pro A:61 Thr A:56 Ser A:59 Leu A:22 Arg A:32 Arg A:28 Gln A:35
4b	Ile A:16 (Carbon) Ile A:7 (Carbon) Tyr A:121 (Carbon)	Leu A:22 (Pi-Sigma) Ile A:60 (Pi-Sigma) Phe A:31 (Pi-Pi T-shaped) Phe A:34 (Pi-Pi T-shaped)	Phe A:34 Ile A:16 Ala A:9 Tyr A:121 Val A:8	Asn A:64 Pro A:61 Thr A:136 Glu A:30 Trp A:24 Val A:115 Gly A:116 Gly A:117 Thr A:56 Gly A:17 Pro A:23 Gly A:20 Asp A:21 Ser A:59 Leu A:67
TcDHFR-TS (PDB ID: 3HBB), (Chagas disease)				
4a	Tyr B:150 (Conventional) Ile B:144 (Conventional) Ser B:82 (Conventional) Asp B:47 (Carbon)	–	Leu B:90 Ile B:83 Met B:48 Phe B:51 Val B:25 Ala B:27	Thr B:79 Lys B:78 Ser B:39 Phe B:87 Ile B:40 Trp B:42 Val B:44 Val B:26 Gly B:146 Gly B:145

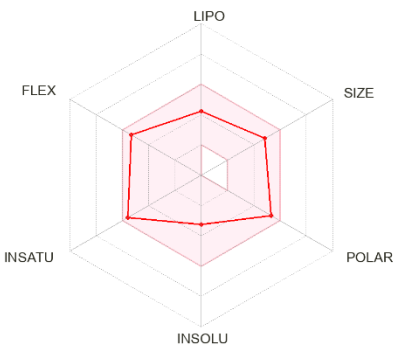
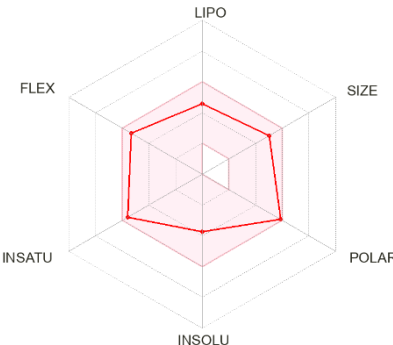
Table 3. Protein-ligand interactions. (Continued)

Compound	Hydrogen Bond	Interactions involved Pi systems	Hydrophobic interactions	Van der Waals interactions
4b	Ala B:27 (Conventional) Val B:26 (Carbon)	–	Phe B:51 Val B:25 Ala B:27 Trp B:42 Ile B:40 Met B:48	Tyr B:150 Ile B:34 Gly B:35 Ser B:39 Arg B:38 Ser B:82 Thr B:79 Asp B:47 Ile B:83 Leu B:90 Ile B:144 Thr B:168
Human DHFR (PDB ID: 1DRF)				
4a	His A:38 (Conventional) Gly A:13 (Carbon) His A:36 (Carbon) Ser A:40 (Carbon)	–	Ala A:15 Ala A:150 Leu A:66	Tyr A:37 Thr A:12 Asn A:109 Pro A:151 Ala A:110 Asn A:147 Ser A:146 Arg A:17 Lys A:16 Arg A:39
4b	His A:38 (Conventional) His A:36 (Carbon) Gly A:13 (Carbon) Ser A:111 (Carbon) Ser A:40 (Carbon)	His A:38 (Pi-Sulfur)	Leu A:66 Ala A:150 Ala A:15	Ser A:67 Ala A:110 Ser A:146 Asn A:147 Pro A:151 Asn A:109 Thr A:12 Tyr A:37 Lys A:16 Arg A:39 Arg A:17

**Fig. 2.** Two- and three-dimensional visualization of interactions at the active site of LdPTR1 (PDBID: 2XOX) protein target and the ligand **4a** and **4b**.

The physicochemical properties of compounds **4a** and **4b** were evaluated using the SwissADME online tool.²¹ Both derivatives complied with the Lipinski,²² Ghose,²³ Veber,²⁴ Egan,²⁵ Muegge²⁶ rules and showed no PAINS alert,²⁷ suggesting their suitability as potential drug candidates.

Table 4. Predicted drug-likeness, ADME-Tox Parameters, and toxicity profiles of the Compounds **4a** and **4b** using web tools.^{21,28,29,30}

Parameters	Compound 4a	Compound 4b	
Bioavailability radar			
	Water solubility, log mol/L	-3.626	-3.798
	LogP	1.82	2.32
	Rotatable Bonds	8	8
	Acceptors	7	6
	Donors	2	2
TPSA, Å ²	111.55	126.57	
Absorption and distribution			
Caco2 permeability, log P _{app} in 10 ⁻⁶ cm/s	1.349	1.427	
Intestinal absorption (human), % Absorbed	83.552	81.42	
Skin Permeability, log K _p	-2.81	-2.854	
VD _{ss} (human), log L/kg	-0.295	-0.135	
CNS permeability, log PS	-3.104	-3.072	
Renal OCT2 substrate, Yes/No	No	No	
Toxicity			
AMES toxicity, Yes/No	No	No	
Max. tolerated dose (human), log mg/kg/day	0.461	0.388	
Predicted Toxicity Class, LD ₅₀	3 LD ₅₀ = 200 mg/kg	3 LD ₅₀ = 250 mg/kg	
Hepatotoxicity, Yes/No	Yes	Yes	
Skin Sensitisation, Yes/No	No	No	
Minnnow toxicity, log mM	-0.089	-0.245	
Mutagenicity	Low risk	Low risk	
Tumorigenicity	Low risk	Low risk	
Irritant effects	Low risk	Low risk	
Reproductive effects	Medium risk	Medium risk	

For each tested compound, a bioavailability radar plot was generated and summarised in **Table 4**, where the pink area represents the optimal physicochemical range for oral bioavailability. This includes lipophilicity (XLOGP3 between -0.7 and +5.0), size (molecular weight between 150 and 500 g/mol), polarity (topological polar surface area, TPSA, between 20 and 130 Å²), solubility (log S ≤ 6), saturation (fraction of sp³-hybridised carbons ≥ 0.25), and flexibility (no more than 9 rotatable bonds).²⁴ All parameters of both compounds fall within these optimal ranges, suggesting good membrane permeability and favourable absorption characteristics.

The BOILED-Egg plot (see **Fig. 5**) demonstrates that the tested compounds are predicted to be absorbed in the gastrointestinal tract (white region), while not permeating the blood–brain barrier (yellow region). Both compounds were found to be actively effluxed by P-glycoprotein, represented as (PGP+), which is indicated by the blue colour of the indicator of the compound. **Table 4** also presents the results of the absorption and distribution evaluation of these compounds. The high Caco2 permeability of both compounds indicates their potential for oral bioavailability. The compounds will be able to penetrate the skin but are unable to penetrate the central nervous system. The volume of distribution is low, which means that the compounds will be distributed more in the plasma than in the tissues. These compounds are not Renal OCT2 substrates.

We also assessed the toxicity of the analyzed compounds (see **Table 4**). The pkCSM web tool²⁸ predicts that they have no Ames toxicity, which means that these compounds are not expected to exhibit mutagenicity and carcinogenicity. The results of the OSIRIS Property Explorer²⁹ also confirm that the analysed compounds are not mutagenic, carcinogenic, or irritating. The toxicity of the Flathead Minnow is not predicted. It should be noted that both compounds are predicted to have a medium risk of reproductive effects and are likely to be hepatotoxic. The analysed compounds are classified as toxicity class 3 according to the ProTox 3.0 webserver.³⁰

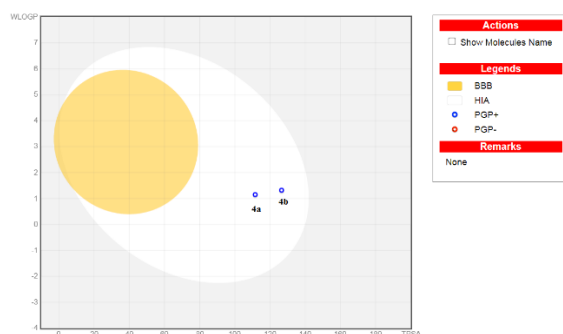


Fig. 5. BOILED-Egg plot for compounds **4a,b**.

3. Conclusions

In this study, novel 4-[3-(ethoxycarbonyl)-1-phenyl-1*H*-pyrazol-4-yl]-2-oxo/thiooxo-1,2,3,4-tetrahydropyrimidine-5-carboxylates were synthesised starting from ethyl 4-formyl-1-phenyl-1*H*-pyrazole-3-carboxylate via multicomponent Biginelli reactions. Molecular docking studies were performed on pteridine reductase 1 (PTR1) of *Leishmania*, dihydrofolate reductase–thymidylate synthase of *Trypanosoma cruzi*, and human dihydrofolate reductase to identify key amino acid residues involved in ligand binding. Furthermore, the absorption, distribution, metabolism, and excretion (ADME) parameters of the synthesised compounds were predicted, enabling an evaluation of their potential safety profiles as drug candidates.

Acknowledgements

This work was financially supported by the Ministry of Education and Science of Ukraine and the Simons Foundation (SFI-PD-Ukraine-00014574).

4. Experimental

4.1. Materials and Methods

The ¹H-NMR spectra presented in this work were obtained on a Varian instrument at an operating frequency of 400 MHz, solvent – DMSO-*d*₆, internal standard – tetramethylsilane. The docking studies were performed using the Autodock Vina³¹ and Discovery Studio³² software packages. Melting points were determined using a Boetius melting point apparatus.

4.2. General procedure

4-[3-(ethoxycarbonyl)-1-phenyl-1*H*-pyrazol-4-yl]-2-oxo/thiooxo-1,2,3,4-tetrahydropyrimidine-5-carboxylates **4a,b**

A mixture of 0.5 g (2 mmol) of ethyl 4-formyl-1-phenyl-1*H*-pyrazole-3-carboxylate, ethyl acetoacetate, and urea or thiourea, each in equimolar amounts (2 mmol), was dissolved in ethanol (10 mL) and refluxed for 6 h. The progress of the reaction was monitored by thin-layer chromatography (TLC). After cooling to room temperature, the reaction mixture was poured into distilled water (30 mL). The precipitated solid was filtered, washed with water, and dried. The crude product was purified by recrystallization from an ethanol–dimethylformamide (EtOH–DMF) mixture.

4.3 Physical and Spectral Data

Ethyl 4-[3-(ethoxycarbonyl)-1-phenyl-1*H*-pyrazol-4-yl]-2-oxo-1,2,3,4-tetrahydropyrimidine-5-carboxylate **4a.** Yield 83%, beige powder, m.p. 235–236 °C. ¹H-NMR (400 MHz, DMSO-*d*₆) δ 9.23 (s, 1H, NH), 8.35 (s, 1H, NH), 7.89 (d, *J* = 8.1 Hz, 2H, Ph), 7.52 (t, *J* = 7.8 Hz, 2H, Ph), 7.38 (t, *J* = 7.2 Hz, 1H, Ph), 7.23 (s, 1H, pyrazole), 5.76 (d, *J* = 2.5 Hz, 1H, CH), 4.45 – 4.28 (m, 2H, EtO), 4.03 – 3.86 (m, 2H, EtO), 2.32 (s, 3H, CH₃), 1.35 (t, *J* = 7.1 Hz, 3H, EtO), 1.03 (t, *J* = 7.1 Hz, 3H, EtO). Found, %: C 60.11; H 5.62; N 14.14. C₂₀H₂₂N₄O₅. Calculated, %: C 60.29; H 5.57; N 14.06.

Ethyl 4-[3-(ethoxycarbonyl)-1-phenyl-1*H*-pyrazol-4-yl]-6-methyl-2-thiooxo-1,2,3,4-tetrahydropyrimidine-5-carboxylate **4b.** Yield 68%, beige powder, m.p. 210–211 °C. ¹H-NMR (400 MHz, DMSO-*d*₆) δ 10.34 (s, 1H, NH), 9.22 (s,

1H, NH), 8.42 (s, 1H, pyrazole), 7.90 (d, $J = 8.3$ Hz, 2H, Ph), 7.53 (t, $J = 7.6$ Hz, 2H, Ph), 7.39 (t, $J = 7.3$ Hz, 1H, Ph), 5.84 (d, $J = 2.4$ Hz, 1H, CH), 4.42 – 4.31 (m, 2H, EtO), 4.01 – 3.90 (m, 2H, EtO), 2.35 (s, 3H, CH₃), 1.35 (t, $J = 7.0$ Hz, 3H, EtO), 1.03 (t, $J = 7.1$ Hz, 3H, EtO). Found, %: C 58.05; H 5.30; N 13.63. C₁₂H₁₃N₅O. Calculated, %: C 57.96; H 5.35; N 13.52.

References

1. Chandravarkar A., Aneja T., Anilkumar G., et al. (2024) Advances in Biginelli reaction: A comprehensive review. *J. Heterocycl. Chem.*, 61 (1), 5–28.
2. Heravi M. M., Asadi S., and Lashkariani B. M. (2013) Recent progress in asymmetric Biginelli reaction. *Mol Divers*, 17 (2), 389–407.
3. Wan J.-P. and Liu Y. (2010) Synthesis of Dihydropyrimidinones and Thiones by multicomponent Reactions: Strategies Beyond the Classical Biginelli Reaction. *Synthesis*, 2010 (23), 3943–3953.
4. Vakhula A. R., Horak Yu. I., Lytvyn R. Z., Lesyuk A. I., Kinzhybalov V., Zubkov F. I., Obushak M. D. (2018) 5-Aryl-2-furaldehydes in the synthesis of tetrahydropyrimidinones by Biginelli reaction. *Chem. Heterocycl. Compd.*, 54 (5), 545–549.
5. Török B., Schäfer C., and Kokel A. (2022) Multicomponent reactions, in: Török B., Schäfer C., and Kokel A. (Eds) *Advances in Green and Sustainable Chemistry. Heterogeneous Catalysis in Sustainable Synthesis*. Elsevier, Amsterdam, 443–489.
6. Dömling A., Wang W., and Wang K. (2012) Chemistry and biology of multicomponent reactions. *Chem. Rev.*, 112 (6), 3083–3135.
7. Herrera R. P., and Marqués-López E. (2015) *Multicomponent Reactions: Concepts and Applications for Design and Synthesis*. Wiley-VCH, Weinheim.
8. John S. E., Gulati S., and Shankaraiah N. (2021) Recent advances in multi-component reactions and their mechanistic insights: a triennium review. *Org. Chem. Front.*, 8 (15) 4237–4287.
9. Graziano G., Stefanachi A., Contino M., Prieto-Díaz R., Ligresti A., Kumar P., Scilimati A., Sotelo E., and Leonetti F. (2023) Multicomponent reaction-assisted drug discovery: a time- and cost-effective green approach speeding up identification and optimization of anticancer drugs. *Int. J. Mol. Sci.*, 24 (7), 6581. (DOI: 10.3390/ijms24076581).
10. Halim K. N. M., Rizk S. A., El-Hashash M. A., and Ramadan S. K. (2020) Straightforward synthesis, antiproliferative screening, and density functional theory study of some pyrazolopyrimidine derivatives. *J. Heterocycl. Chem.*, 58 (2), 636–645.
11. Bhatt J. D., Chudasama C. J., and Patel K. D. (2017) Diarylpyrazole ligated dihydropyrimidine hybrids as potent non-classical antifolates and their efficacy against *Plasmodium falciparum*. *Arch. Pharm. (Weinheim)*, 350 (9), 1700088. (DOI: 10.1002/ardp.201700088).
12. Viveka S., Dinesha, Madhu L. N., and Nagaraja G. K. (2015) Synthesis of new pyrazole derivatives via multicomponent reaction and evaluation of their antimicrobial and antioxidant activities. *Monatsh. Chem.*, 146 (9), 1547–1555.
13. Suresh L., Vijay Kumar P. S., Poornachandra Y., Ganesh Kumar C., and Chandramouli G. V. P. (2016) An efficient one-pot synthesis of thiochromeno[3,4-d]pyrimidines derivatives: Inducing ROS dependent antibacterial and anti-biofilm activities. *Bioorg. Chem.*, 68, 159–165.
14. Trivedi A. R., Bhuvu V. R., Dholariya B. H., Dodiya D. K., Kataria V. B., and Shah V. H. (2010) Novel dihydropyrimidines as a potential new class of antitubercular agents. *Bioorg. Med. Chem. Lett.*, 20 (20), 6100–6102.
15. Yadlapalli R. K., Chourasia O. P., Vemuri K., Sritharan M., and Perali R. S. (2012) Synthesis and in vitro anticancer and antitubercular activity of diarylpyrazole ligated dihydropyrimidines possessing lipophilic carbamoyl group. *Bioorg. Med. Chem. Lett.*, 22 (8), 2708–2711.
16. Fahmy H. H., Khalifa N. M., Nossier E. S., Abdalla M. M., and Ismail M. M. F. (2012) Synthesis and anti-inflammatory evaluation of new substituted 1-(3-chlorophenyl)-3-(4-methoxyphenyl)-1H-pyrazole derivatives. *Acta Pol. Pharm.*, 69 (3), 411–421.
17. Zohny Y. M., Awad S. M., Rabie M. A., and Alsaidan O. A. (2023) Design, Synthesis, Molecular Modeling, and Biological Evaluation of Novel Pyrimidine Derivatives as Potential Calcium Channel Blockers. *Molecules*, 28 (12), 4869. (DOI: 10.3390/molecules28124869)
18. Halim K. N. M., Rizk S. A., Ramadan S. K., and El-Hashash M. A. (2020) Synthesis, DFT study, molecular docking and insecticidal evaluation of some pyrazole-based tetrahydropyrimidine derivatives. *Synth. Commun.*, 50 (8), 1159–1169. (DOI: 10.1080/00397911.2020.1720739)
19. MolPredictX. Available online. <https://www.molpredictx.ufpb.br/home/> (accessed on 10 July 2025).
20. Neves G. M., Kagami L. P., Gonçalves I. L., and Eifler-Lima V. L. (2019) Targeting pteridine reductase 1 and dihydrofolate reductase: the old is a new trend for leishmaniasis drug discovery. *Future Med. Chem.*, Epub ahead of print. (DOI: 10.4155/fmc-2018-0512).
21. SwissADME. Available online: <http://www.swissadme.ch/index.php> (accessed on 10 July 2025).
22. Lipinski C.A., Lombardo F., Dominy B.W., Feeney P.J. (1997) Experimental and computational approaches to estimate solubility and permeability in drug discovery and development settings. *Adv. Drug Deliv. Rev.*, 23(1-3), 3-25. (DOI: 10.1016/S0169-409X(96)00423-1).

23. Ghose A.K., Viswanadhan V.N., Wendoloski J.J. (1999) A knowledge-based approach in designing combinatorial or medicinal chemistry libraries for drug discovery. 1. A qualitative and quantitative characterization of known drug databases. *J. Comb. Chem.*, 1(1), 55-68.
24. Veber D.F., Johnson S.R., Cheng H.Y., Smith B.R., Ward K.W., Kopple K.D. (2002) Molecular properties that influence the oral bioavailability of drug candidates. *J. Med. Chem.*, 45(12), 2615-2623.
25. Egan W.J., Merz K.M. Jr., Baldwin J.J. (2000) Prediction of drug absorption using multivariate statistics. *J. Med. Chem.*, 43(21), 3867-3877.
26. Muegge I., Heald S.L., Brittelli D. (2001) Simple selection criteria for drug-like chemical matter. *J. Med. Chem.*, 44(12), 1841-1846.
27. Vidler L.R., Maan Dutta M., Talukdar H., Phukan P., Mader M.M., Strelow J.M., Mader M.M., Evans D., Strelow J.M. (2018) Investigating the behavior of published PAINS alerts using a large-scale screening dataset. *ACS Med. Chem. Lett.*, 9(8), 792–796.
28. Pharmacokinetic properties. Available online: <https://biosig.lab.uq.edu.au/pkcsm/prediction> (accessed on 10 July 2025).
29. OSIRIS Property Explorer. Available online: <https://www.organic-chemistry.org/prog/peo/> (accessed on 10 July 2025).
30. ProTox 3.0 – Prediction Of Toxicity Of Chemicals programme. Available online: <https://tox.charite.de/protox3/index.php?site=home> (accessed on 10 July 2025).
31. Autodock Vina. <https://vina.scripps.edu/> (accessed on 10 July 2025).
32. Discovery Studio. <https://discover.3ds.com/discovery-studio-visualizer-download> (accessed on 10 July 2025).



© 2025 by the authors; licensee Growing Science, Canada. This is an open access article distributed under the terms and conditions of the Creative Commons Attribution (CC-BY) license (<http://creativecommons.org/licenses/by/4.0/>).